

(*p, d*³He) reaction as a quasifree reaction process*

A. A. Cowley,[†] P. G. Roos, N. S. Chant, R. Woody, III,[‡] H. D. Holmgren, and D. A. Goldberg

Department of Physics and Astronomy, University of Maryland, College Park, Maryland 20742

(Received 29 November 1976)

The (*p, d*³He) reaction of ⁶Li, ⁷Li, ⁹Be, and ¹²C has been investigated in conjunction with studies of the (*p, pα*) reaction on the same targets. Coincident data for all four targets were obtained at a bombarding energy of 100 MeV for numerous angle pairs in order to test the reaction mechanism. Comparisons of the (*p, d*³He) data to both (*p, pα*) data and distorted-wave impulse approximation calculations indicate a dominance of the direct quasifree reaction process (*p + α → d + ³He*). The absolute α-particle spectroscopic factors extracted using distorted-wave impulse approximation analysis are in agreement with the values obtained in the (*p, pα*) reaction.

NUCLEAR REACTIONS ⁶Li, ⁷Li, ⁹Be, ¹²C (*p, d*³He), *E*₀=100 MeV; measured $d^3\sigma/d\Omega_d d\Omega_{^3\text{He}} dE_d(\theta_d, \theta_{^3\text{He}}, E_d)$; coplanar geometry; DWIA analysis; deduced α-particle spectroscopic factors.

I. INTRODUCTION

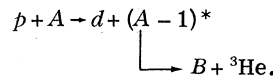
In a previous paper¹ we presented a detailed experimental study of the (*p, pα*) reaction on four 1*p*-shell nuclei. These data provided strong evidence for the interpretation of the (*p, pα*) reaction at 100 MeV as a quasifree α-particle knockout reaction. Moreover, a distorted-wave impulse approximation (DWIA) analysis^{1,2} of the data provided absolute α-particle spectroscopic factors which agreed with theoretical predictions. In conjunction with the experimental work on the (*p, pα*) reaction, data were also obtained for the (*p, d*³He) reaction to test its possible interpretation in terms of a quasifree reaction process; several other experimental studies³⁻⁶ have suggested the importance of such a process in three-body final state reactions.

To illustrate what we mean by the term "quasifree reaction" let us compare the two reactions *A(p, pα)B* and *A(p, d³He)B*. In Fig. 1 we present for these reactions the first order diagrams which we assume represent the dominant processes in the region of interest. We see that the reactions differ only in the upper vertex, which in the first case represents elastic *p-α* scattering and in the second case represents the ⁴He(*p, d*)³He reaction. It is the nature of the respective upper vertices which give rise to our use of the terms quasifree elastic scattering and quasifree reaction.

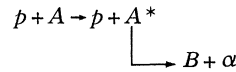
Assuming that the first order diagram dominates and that the corrections to it are adequately treated using DWIA, then, based on Fig. 1, we would expect to obtain identical nuclear structure information from the (*p, pα*) and (*p, d*³He) reactions. Since generally the quasifree elastic scat-

tering cross section is larger than the quasifree reaction cross section by approximately the ratio of the two-body cross sections associated with the upper vertex, it would appear to be experimentally advantageous to study the former process. Thus before presenting the results it is worthwhile suggesting several important reasons for studying such quasifree reactions.

Firstly, a practical reason is that there appear to be no significant contributions due to sequential events of the type



In contrast, for (*p, pα*) near 100 MeV the sequential processes



create some difficulty¹ and require that the experiments be carried out at relatively large proton angles (generally $\theta_p > 75^\circ$) where the cross sections are small, in order to prevent contamination of the quasifree peak by the sequential processes. Thus one generally obtains much cleaner quasifree reaction spectra at the expense of somewhat longer running times.

Secondly, the comparison of the (*p, d*³He) and (*p, pα*) reactions may provide additional information on the four-particle structure in the target nucleus and/or detailed information on the *p + α*-cluster interaction. For example, if we consider the four-particle internal structure in the target nucleus as a superposition of the α ground-state configuration plus excited states of the α particle, then the (*p, pα*) reaction can in principle occur

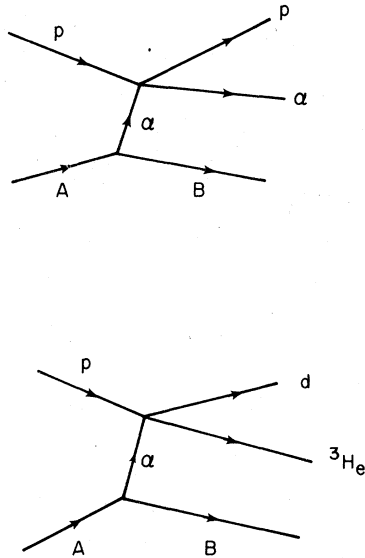


FIG. 1. First order diagrams for the $A(p, p\alpha)B$ and $A(p, d^3\text{He})B$ reactions.

not only through $p - \alpha$ elastic scattering but also via proton inelastic scattering from the excited states to the α -particle ground state. In the $(p, d^3\text{He})$ reaction similar effects should be present. A detailed comparison of the two reactions may then elucidate the importance of such effects. An attempt to utilize this feature of the quasifree reaction has been made by Grossiord *et al.*⁴ who have studied the ${}^6\text{Li}(d, tp){}^4\text{He}$ reaction in order to obtain information on the deuteron deformation in ${}^6\text{Li}$. A theoretical attempt to include the scattering from excited states of the " α " cluster to the ground state by means of Glauber theory has also been made.⁷ However, distortion effects due to the residual nucleus B would have to be included in the calculations before reaching any definitive conclusions concerning the importance of these terms.

In the present paper we present extensive experimental data for the $(p, d^3\text{He})$ reaction on the same p -shell targets (${}^6\text{Li}$, ${}^7\text{Li}$, ${}^9\text{Be}$, and ${}^{12}\text{C}$) studied with the $(p, p\alpha)$ experiment. These data provide independent tests of the reaction mechanism (i.e., tests of the dominance of the quasifree reaction mechanism). We also make direct comparisons to the $(p, p\alpha)$ data to ascertain the similarity of the two reactions as would be expected from the diagrams presented in Fig. 1 and direct comparisons with DWIA calculations.

II. THEORY

In the plane-wave impulse approximation (PWIA) expression corresponding to the two diagrams in

Fig. 1, the triple differential cross section for both quasifree elastic scattering and quasifree reactions can be expressed in identical form as

$$\frac{d^3\sigma}{d\Omega_1 d\Omega_2 dE_1} = \text{K.F.} \cdot \frac{d\sigma}{d\Omega} \Big|_{1-2} S_\alpha |\phi(-\vec{p}_B)|^2, \quad (1)$$

where K.F. is a known kinematic factor and $d\sigma/d\Omega|_{1-2}$ is the (off-energy-shell) two-body cross section [$p - \alpha$ elastic scattering for $(p, p\alpha)$ and ${}^4\text{He}(p, d){}^3\text{He}$ for the $(p, d^3\text{He})$ reaction]. The quantity S_α is an α -particle spectroscopic factor, and $\phi(-\vec{p}_B)$ represents the lower vertex which is common to both reactions. This latter quantity is the Fourier transform of the overlap integral between the internal wave function of the target nucleus A and the internal wave functions of the residual nucleus B and the α particle (i.e., it is basically the momentum space wave function of the α cluster in the nucleus) and is normalized to unity. The momentum \vec{p}_B is the recoil momentum of the residual nucleus, a quantity which can be deduced from the experimental measurements. Based on the first order diagrams and the PWIA expression given in Eq. (1), it is clear that the two reactions in principle contain identical nuclear structure information on α clustering in the target nucleus.

For the $(p, p\alpha)$ reaction we have shown that the PWIA interpretation is inadequate for quantitative comparisons, but that most of the gross features predicted by the PWIA are evident in the data. This result suggested that one could assume the dominance of the first order $(p, p\alpha)$ diagram and include distortion effects due to the residual nucleus B via the distorted-wave impulse approximation (DWIA). The resultant DWIA calculations for the $(p, p\alpha)$ reaction provided excellent agreement with the experimental data. One expects similar results for the $(p, d^3\text{He})$ reactions.

The DWIA formalism for the general reaction of the type $A(a, cd)B$ has been developed by Chant and Roos.^{2,8} The inclusion of distortion effects with the DWIA preserves the form of Eq. (1) for both reactions and modifies only the ϕ^2 term of the PWIA expression [Eq. (1)] replacing it by the distorted momentum distribution

$$|\phi(-\vec{p}_B)|^2 = \sum_A |T_{BA}^{\alpha L A}|^2, \quad (2)$$

where the amplitude $T_{BA}^{\alpha L A}$ is given by

$$T_{BA}^{\alpha L A} = \frac{1}{(2L+1)^{1/2}} \int \chi_d^{(-)*}(\vec{r}) \chi_c^{(-)*}(\vec{r}) \chi_a^{(+)}(\gamma\vec{r}) \times \phi_{LA}^\alpha(\vec{r}) d\vec{r}. \quad (3)$$

The χ 's represent distorted waves for the incoming and outgoing particles, $\gamma = A/B$ and $\phi_{LA}^\alpha(\vec{r})$ is the coordinate-space wave function of the α

cluster. The inclusion of distortion has been shown^{1, 2, 6, 8} to produce large effects in cluster knockout reactions, even up to energies of order 600 MeV, and must be included in order to extract any quantitative nuclear structure information from such reactions.

III. EXPERIMENT

The experimental arrangement has been described in detail in our previous paper¹ on the $(p, p\alpha)$ reaction which was performed simultaneously. Briefly, a 100 MeV proton beam from the University of Maryland cyclotron was focused on targets placed at the center of a 150 cm diam scattering chamber. The outgoing particles were detected by two detector telescopes placed coplanar with and on opposite sides of the incident beam. The detector telescope for p , d , and t consisted of a 1 mm Si surface barrier ΔE , followed by a 2.5 cm diam \times 5 cm thick NaI(Tl) crystal ($\Delta\Omega = 4.83$ msr); the telescope for ${}^3\text{He}$ and ${}^4\text{He}$ consisted of a 200 μm Si surface barrier ΔE followed by a 3 mm Si(Li) E detector ($\Delta\Omega = 1.21$ msr). Conventional electronics were used and five linear signals, gated by appropriate logic signals, were sent to analog-to-digital converters interfaced to an on-line IBM 360/44 computer. These linear signals consisted of the two ΔE outputs, the two E outputs, and a time-to-amplitude converter output which measured the time difference between the two ΔE signals (with a resolving time of approximately 1.5 ns) allowing the simultaneous storage of real and accidental coincidence events. Software data handling was performed by the versatile code⁹ P2P. Further experimental details can be found in Ref. 1.

Since we wished to investigate the appropriateness of the DWIA equivalent of Fig. 1, angle pairs $(\theta_p, \theta_{{}^3\text{He}})$ were generally chosen such that the residual undetected nucleus B was left with relatively small recoil momentum \vec{p}_B . For each target except ${}^{12}\text{C}$, primary emphasis was placed on the one angle pair $(\theta_p = \theta_d \simeq 81^\circ, \theta_\alpha = \theta_{{}^3\text{He}} \simeq -41^\circ)$ which for both the $(p, p\alpha)$ and $(p, d{}^3\text{He})$ reactions corresponded to quasifree angle pairs; i.e., in both reactions zero recoil momentum of the residual nucleus was kinematically allowed at that same angle pair. In the following we refer to this particular set of angles as the "double quasifree angle pair." At these angles the simultaneous accumulation of data for the two reactions provided the most complete comparison (maximum range of recoil momentum), and is free of most relative errors. For ${}^{12}\text{C}$, data were obtained only at $(p, p\alpha)$ quasifree angle pairs. However, the minimum recoil momentum for the $(p, d{}^3\text{He})$ reaction was still

sufficiently small to allow a useful comparison of the two reactions.

Data at additional angle pairs were obtained, providing further tests of the reaction mechanism. Most of these angle pairs corresponded to $(p, p\alpha)$ quasifree angle pairs, although the minimum recoil momenta for $(p, d{}^3\text{He})$ were still relatively small. For ${}^6\text{Li}(p, d{}^3\text{He}){}^2\text{H}$ a series of quasifree angle pair data were obtained in order to study the angular dependence of the zero recoil momentum point ($\vec{p}_B = 0$). These data provide a test of the factorization approximation made in the DWIA.

IV. EXPERIMENTAL RESULTS

A variety of experimental results have been obtained and in the following subsections we present not only the $(p, d{}^3\text{He})$ results, but also make detailed comparisons with the $(p, p\alpha)$ data which have been shown to be in excellent agreement with the DWIA knockout theory. Although many of the presentations of the data contain overlapping information, the breakdown most clearly separates various features of the reactions.

A. Binding energy spectra

Consider a reaction of the type $A(a, cd)B$ in which the energies of the outgoing particles c and d are measured at (θ_c, θ_d) . From these data one can calculate the binding energy $F_3 = E_c + E_d + E_B = E_a + Q + E^*$ where the E_i are the energies of the various particles (E_B , the energy of the undetected recoiling nucleus, is calculated from the three-body kinematics), Q is the ground state Q value of the reaction, and E^* is the excitation energy in the residual nucleus B . A plot of the number of coincident events versus $E^* = E_a + Q - F_3$ represents the probability of excitation of the various states in the final nucleus. If the concepts of quasifree elastic scattering and quasifree reactions (as represented by Fig. 1) have any validity then the excitation energy spectra of the $(p, p\alpha)$ and $(p, d{}^3\text{He})$ reactions should be nearly identical. Small differences might be expected from such effects as differing distortions in the two types of reactions, and differing energy dependence in the two-body cross sections $d\sigma/d\Omega|_{1-2}$, and from the experimental restriction that thresholds created by the $\Delta E E$ coincidence requirement in each telescope limit the range of energy sharing contained in the summation. However, we would not expect to observe any major differences.

In Fig. 2 we present the excitation energy spectra for the two reactions on the four target nuclei. For ${}^6\text{Li}$, ${}^7\text{Li}$, and ${}^9\text{Be}$ the angles correspond to

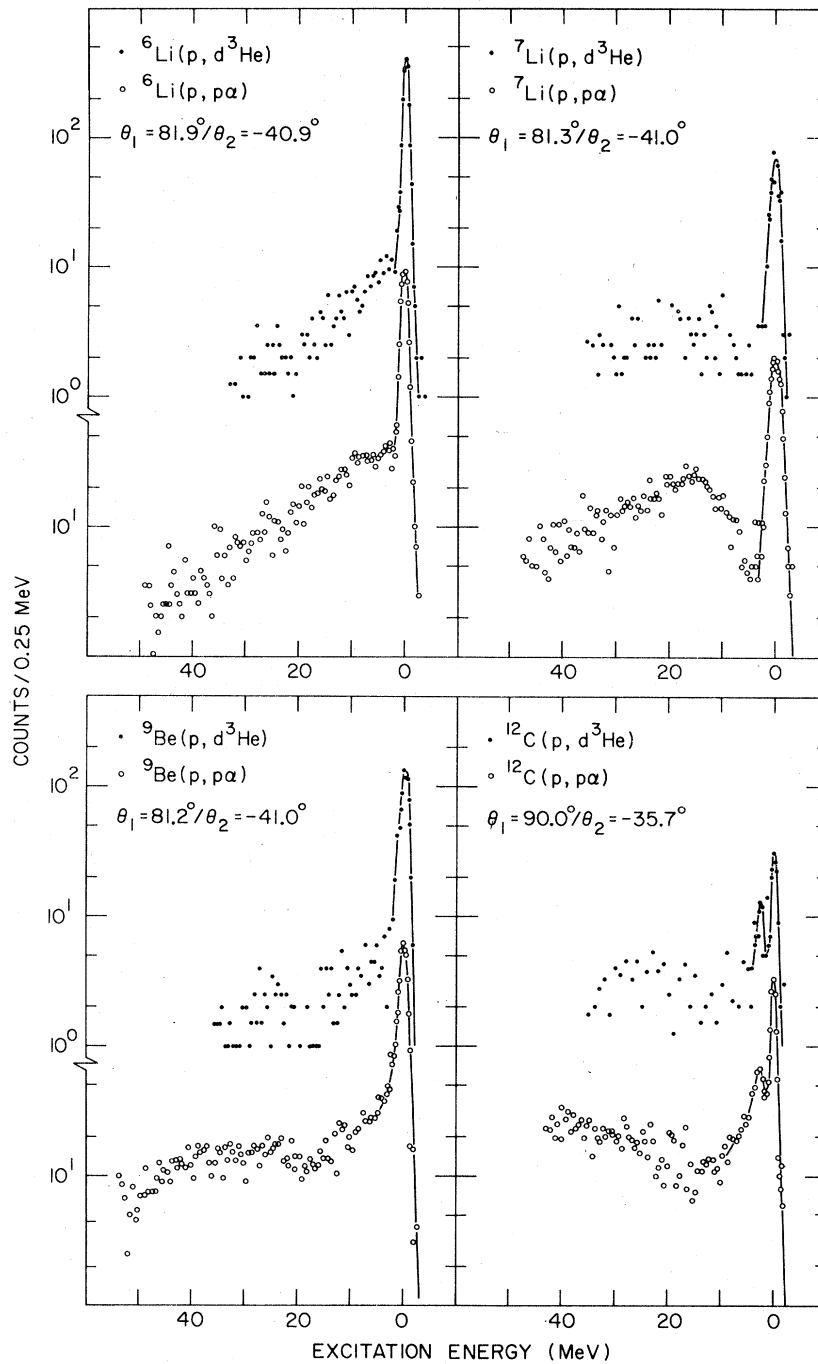


FIG. 2. Binding energy spectra versus excitation energy for the $(p, p\alpha)$ and $(p, d^3\text{He})$ reactions at a bombarding energy of 100 MeV and angle pairs $\theta_p = \theta_d = \theta_1$ and $\theta_\alpha = \theta_{^3\text{He}} = \theta_2$.

quasifree angles, whereas for ^{12}C the angle differs slightly from the quasifree $(p, d^3\text{He})$ angle. We observe that the spectra are basically identical, and that little evidence is seen for excited states beyond that of the 2.9 MeV region in ^9Be .

$$\text{B. Energy sharing } \frac{d^3\sigma}{d\Omega_d d\Omega_{^3\text{He}} dE_d}$$

For each set of angle pairs and each state in the final nucleus we have projected the data onto the

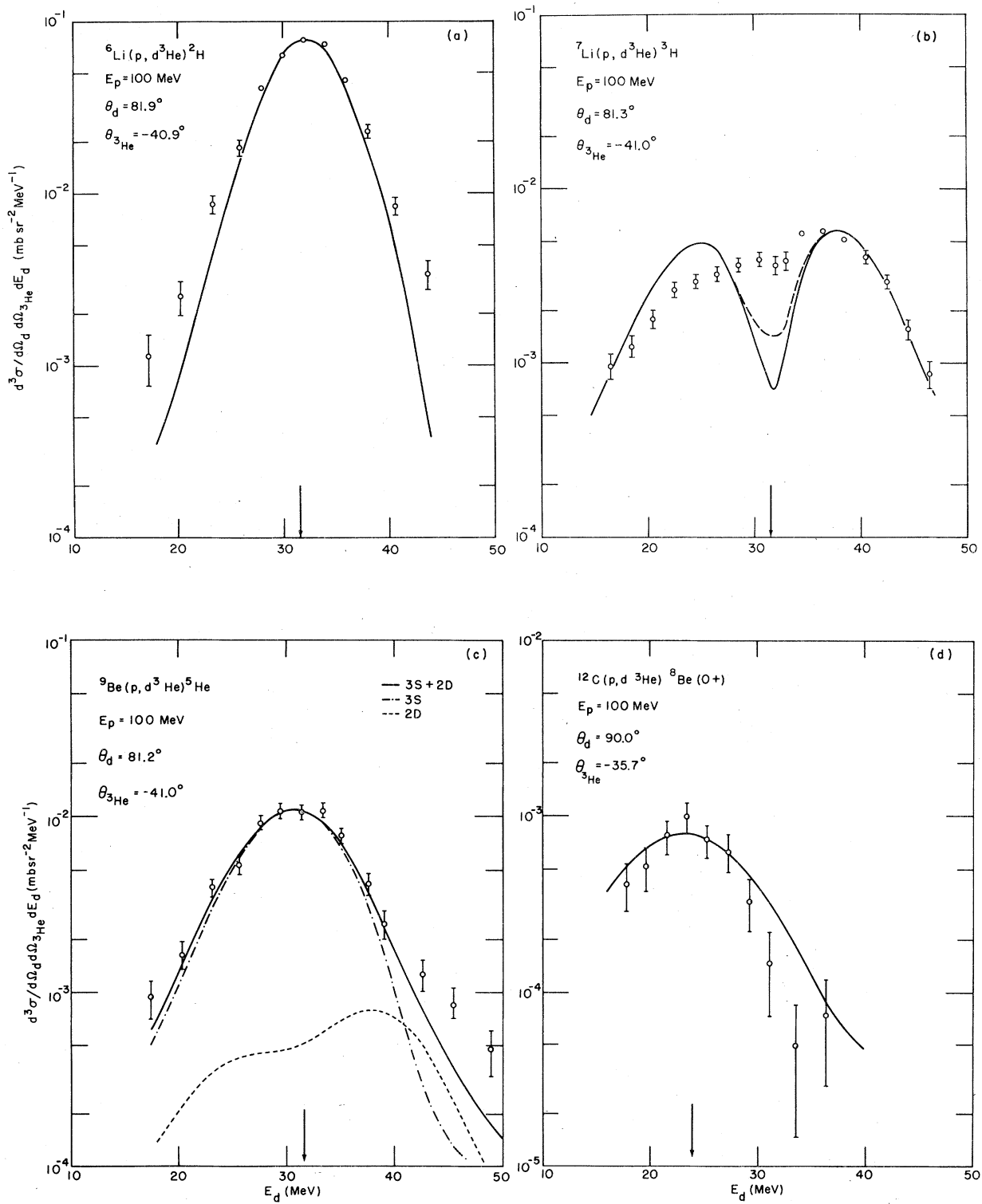


FIG. 3. Three-body cross sections for the (a) ${}^6\text{Li}(p, d^3\text{He}){}^2\text{H}$, (b) ${}^7\text{Li}(p, d^3\text{He}){}^3\text{H}$, (c) ${}^9\text{Be}(p, d^3\text{He}){}^5\text{He}$, and (d) ${}^{12}\text{C}(p, d^3\text{He}){}^8\text{Be}(0^+, \text{g.s.})$ reactions at 100 MeV. The arrows on the deuteron energy axes indicate the locations of zero recoil momentum. The solid curves are DWIA calculations normalized to the data (see Sec. IV). In Fig. (b) the dashed curve includes the effects of the finite experimental angular and energy resolution on the DWIA calculation.

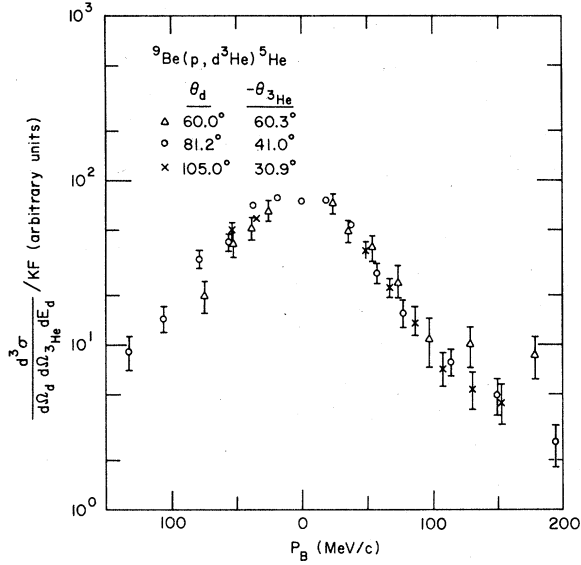


FIG. 4. $(d^3\sigma/d\Omega_d d\Omega_{3\text{He}} dE_d)/\text{K.F.}$ [see Eq. (4)] versus recoil momentum for the ${}^9\text{Be}(p, d^3\text{He}){}^5\text{He}$ reaction at three angle pairs. The different angle pairs have been normalized near $p_B=0$.

deuteron energy axis to obtain the triple differential cross section $d^3\sigma/d\Omega_d d\Omega_{3\text{He}} dE_d$. Typical data for quasifree angles are presented in Fig. 3 along with the DWIA calculations discussed in Sec. V. The deuteron energy corresponding to zero recoil momentum of the undetected residual nucleus is indicated by an arrow on the energy axis. The data for ${}^6\text{Li}-{}^2\text{H}$, ${}^9\text{Be}-{}^5\text{He}$, and ${}^{12}\text{C}-{}^8\text{Be}(0+)$ clearly show the peak at approximately zero recoil momentum expected for the reaction proceeding via the direct (p, d) interaction on an S-state α cluster. For ${}^7\text{Li}(p, d^3\text{He}){}^3\text{H}$, which must proceed via an interaction with a P-state α particle, we see evidence of a slight dip near $\vec{p}_B=0$, but not as pronounced as that observed in the $(p, p\alpha)$ reaction.¹ The data for ${}^{12}\text{C}(p, d^3\text{He}){}^8\text{Be}$ (2.9 MeV region) have been excluded from consideration owing to the presence of mixed angular momentum transfer as discussed in Ref. 1.

As a further test of the quasifree reaction mechanism, we have compared the three-body cross sections divided by the kinematic factor for various quasifree angle pairs. In the DWIA we have

$$\frac{d^3\sigma}{d\Omega_d d\Omega_{3\text{He}} dE_d} / \text{K.F.} = S_\alpha \left. \frac{d\sigma}{d\Omega} \right|_{p=d} \phi_{\text{DW}}^2. \quad (4)$$

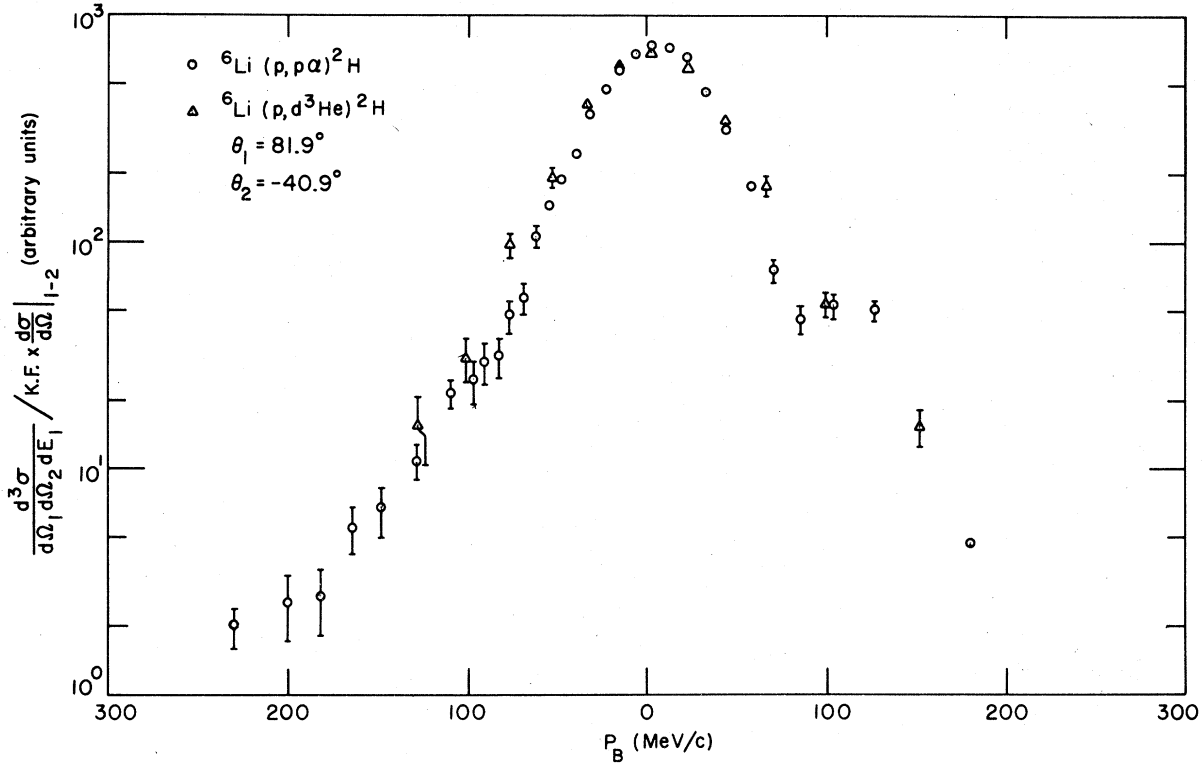


FIG. 5. The ratio $(d^3\sigma/d\Omega_1 d\Omega_2 dE_1)/\text{K.F.} \times d\sigma/d\Omega|_{1-2}$ for the ${}^6\text{Li}(p, p\alpha){}^2\text{H}$ and the ${}^6\text{Li}(p, d^3\text{He}){}^2\text{H}$ reactions. For the $(p, p\alpha)$ reaction $d\sigma/d\Omega|_{1-2}$ has been obtained by interpolation, whereas for the $(p, d^3\text{He})$ reaction a constant $d\sigma/d\Omega|_{1-2}$ has been assumed. The two sets of data have been normalized near $p_B=0$.

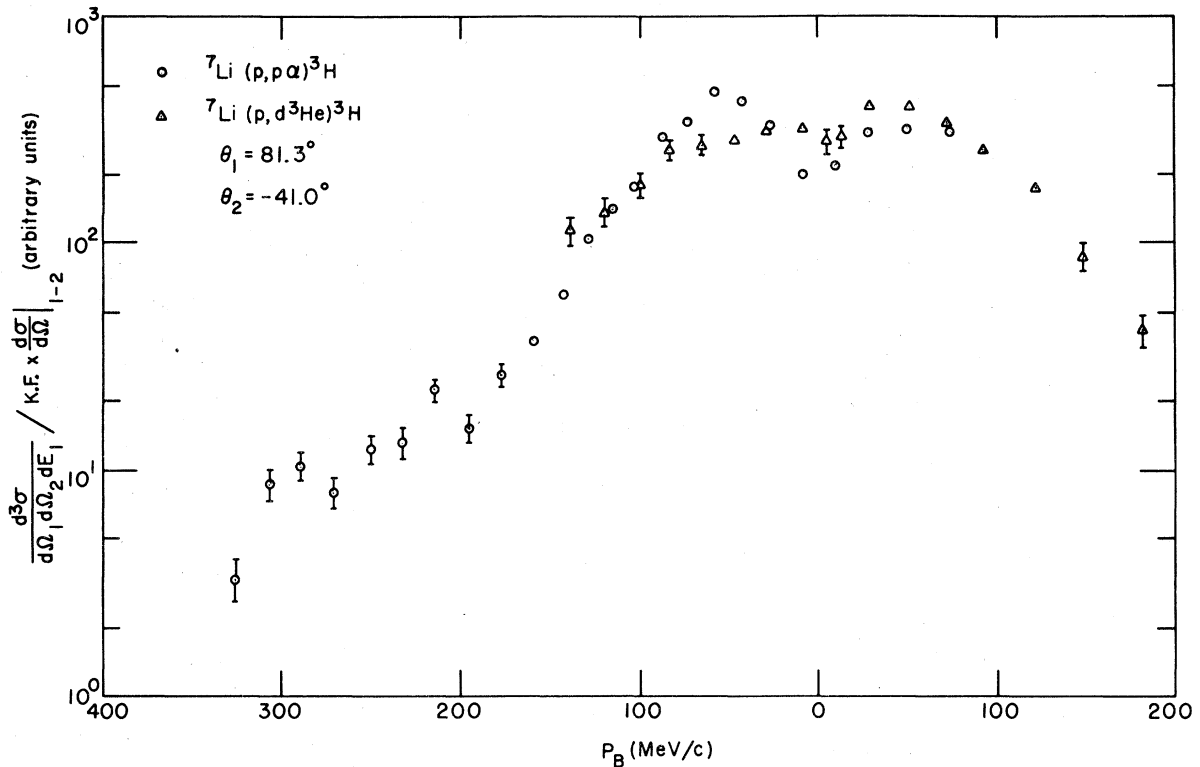


FIG. 6. The ratio $(d^3\sigma/d\Omega_1 d\Omega_2 dE_1)/K.F. \times d\sigma/d\Omega|_{1-2}$ for the ${}^7\text{Li}(p, p\alpha){}^3\text{H}$ and the ${}^7\text{Li}(p, d^3\text{He}){}^3\text{H}$ reactions (see Fig. 5 caption).

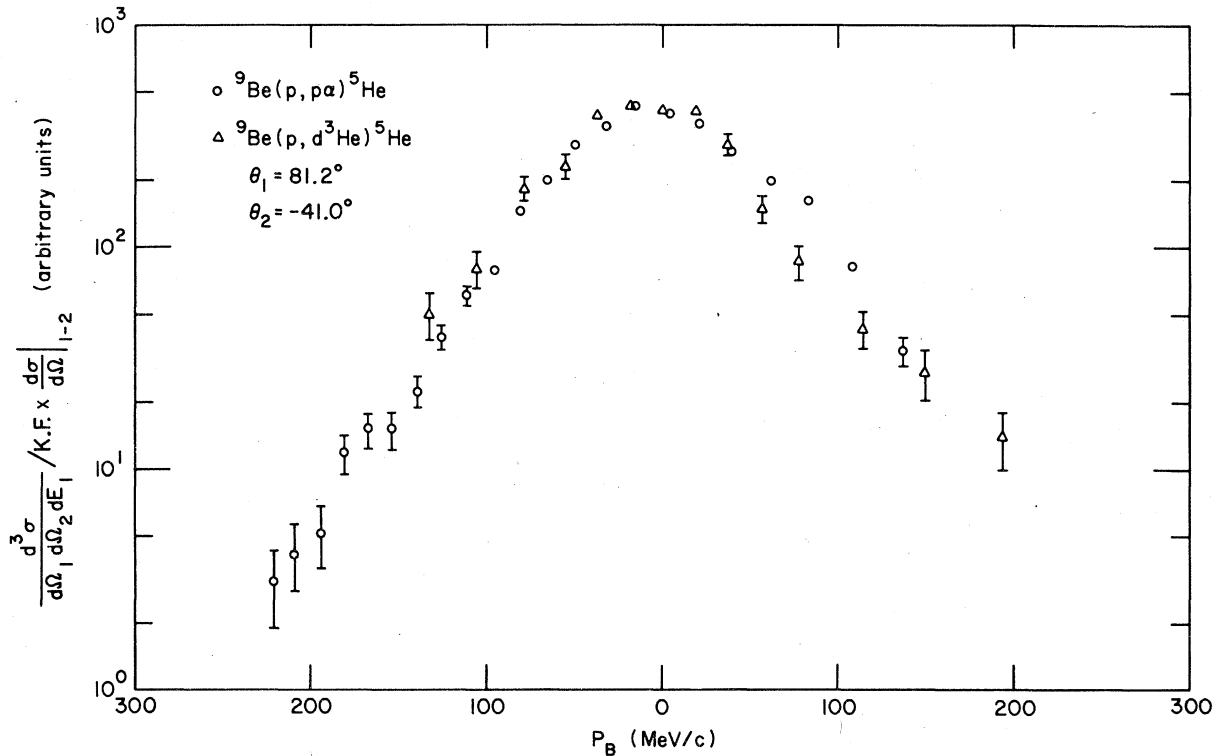


FIG. 7. The ratio $(d^3\sigma/d\Omega_1 d\Omega_2 dE_1)/K.F. \times d\sigma/d\Omega|_{1-2}$ for the ${}^9\text{Be}(p, p\alpha){}^5\text{He}$ and ${}^9\text{Be}(p, d^3\text{He}){}^5\text{He}$ reactions (see Fig. 5 caption).

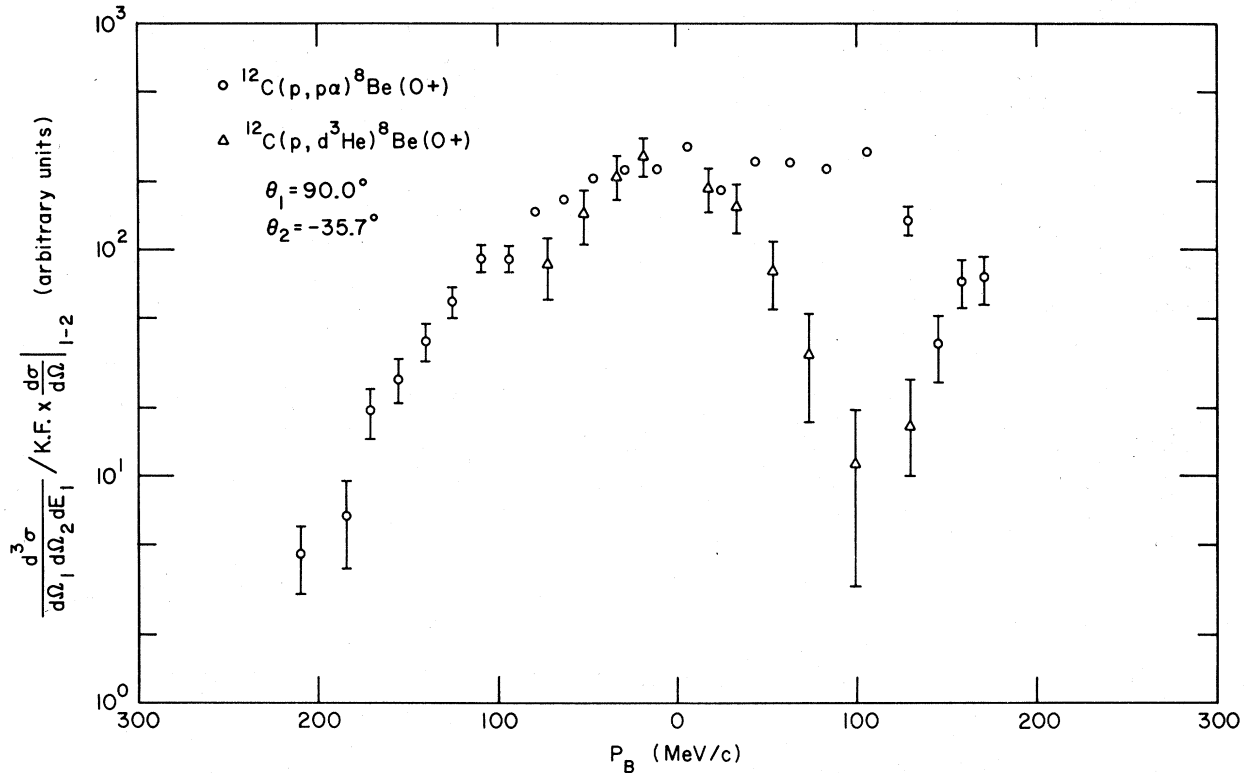


FIG. 8. The ratio $(d^3\sigma/d\Omega_1 d\Omega_2 dE_1)/K.F. \times d\sigma/d\Omega|_{l=2}$ for the $^{12}\text{C}(p, p\alpha)^8\text{Be}(0+)$ and $^{12}\text{C}(p, d^3\text{He})^8\text{Be}(0+)$ reactions (see Fig. 5 caption).

Since explicit DWIA calculations indicate that the distortion effects are not strongly angle and energy dependent and the variation in $d\sigma/d\Omega|_{p-\alpha}$ is small over the energy sharing spectrum, the shape of the quantity defined in Eq. (4) should be angle independent for any particular reaction. In Fig. 4 we present the three-body cross section divided by K.F. versus the measured recoil momentum for the $^9\text{Be}(p, d^3\text{He})^5\text{He}$ reaction. The data for different angles have been normalized near zero recoil momentum. In agreement with DWIA expectations we find nearly identical shapes for the various angles presented. Other targets and angle pairs produce comparable agreement.

Finally, in the spirit of the diagrams given in Fig. 1 comparing the direct $(p, d^3\text{He})$ and $(p, p\alpha)$ reactions, we compare the three-body cross sections divided by $K.F. \times d\sigma/d\Omega$ for the two reactions versus recoil momentum. For $(p, p\alpha)$ the values of $d\sigma/d\Omega|_{p-\alpha}$ were obtained by interpolation of $p-\alpha$ elastic scattering (see Ref. 1), whereas for $(p, d^3\text{He})$ a constant cross section has been used. Interpolation of the available $^4\text{He}(p, d)^3\text{He}$ data¹⁰ shows that the variation is small over the kinematic range of the energy sharing spectrum. For this comparison we have used the data correspond-

ing to the double quasifree angle pair, i.e., the angle pair such that it is kinematically possible for both reactions to leave the residual nucleus at rest. Since these data were taken simultaneously they are free of many relative errors. These comparisons are presented in Figs. 5–8, where the $(p, d^3\text{He})$ results have been normalized to the $(p, p\alpha)$ results near zero recoil momentum. The agreement between the two reactions is quite good, with the exception of the regions in the $(p, p\alpha)$ spectra which contain sequential events (the right hand side of $p_B = 0$), and the region of the minimum in the ^7Li reactions. A discussion of the relative normalization of these two reactions, which depends on both the two-body cross sections and the relative distortion effects, is deferred until Sec. V.

The shapes and intercomparisons of the energy sharing data presented above all point to the dominance of the first order quasifree reaction diagram.

C. Angular distributions

Again assuming relatively constant distortion effects, the factorization of the two-body cross

section assumed in the DWIA implies that the angular dependence of the $(p, d^3\text{He})$ reaction for fixed recoil momentum should be dominated by the angular dependence of the two-body cross section $d\sigma/d\Omega|_{p=d}$. In order to test this assumption we have plotted $(d^3\sigma/d\Omega_d d\Omega_{3\text{He}} dE_d)/K.F.$ for fixed recoil momentum ($p_B \approx 0$ MeV/c) versus the two-body center-of-mass angle calculated for the final state of the three-body system. In the DWIA the angular dependence of this quantity should be essentially the same as the two-body ${}^4\text{He}(p, d){}^3\text{He}$ reaction. Explicit DWIA calculations show that the variation in $|\phi_{\text{DW}}|^2$ over the angular range studied is less than 8%. Unfortunately, only for ${}^6\text{Li}$ is the angular range sufficiently large to provide a satisfactory test. In Fig. 9 we present these results for $p_B \approx 0$ MeV/c. Also presented in Fig. 9 are the available two-body ${}^4\text{He}(p, d){}^3\text{He}$ cross section data.¹⁰

In spite of the lack of free (p, d) data, a comparison with the available data strongly supports the factorization approximation for the ${}^6\text{Li}(p, d^3\text{He}){}^2\text{H}$ reaction. For the other nuclei studied the available data lie in the rather flat portion of the two-body cross section ($\theta \approx 100^\circ - 130^\circ$), and one can only say that the data are consistent with the factorization approximation and the quasifree reaction mechanism concept.

V. DWIA CALCULATIONS

Theoretical calculations for the present $(p, d^3\text{He})$ data have been carried out using the general DWIA code of Chant.^{2,8} The calculations have been described in detail in Refs. 2 and 8. Since our desire is to compare with the previous $(p, p\alpha)$ analysis, we have tried to be as consistent as possible with these previous calculations.

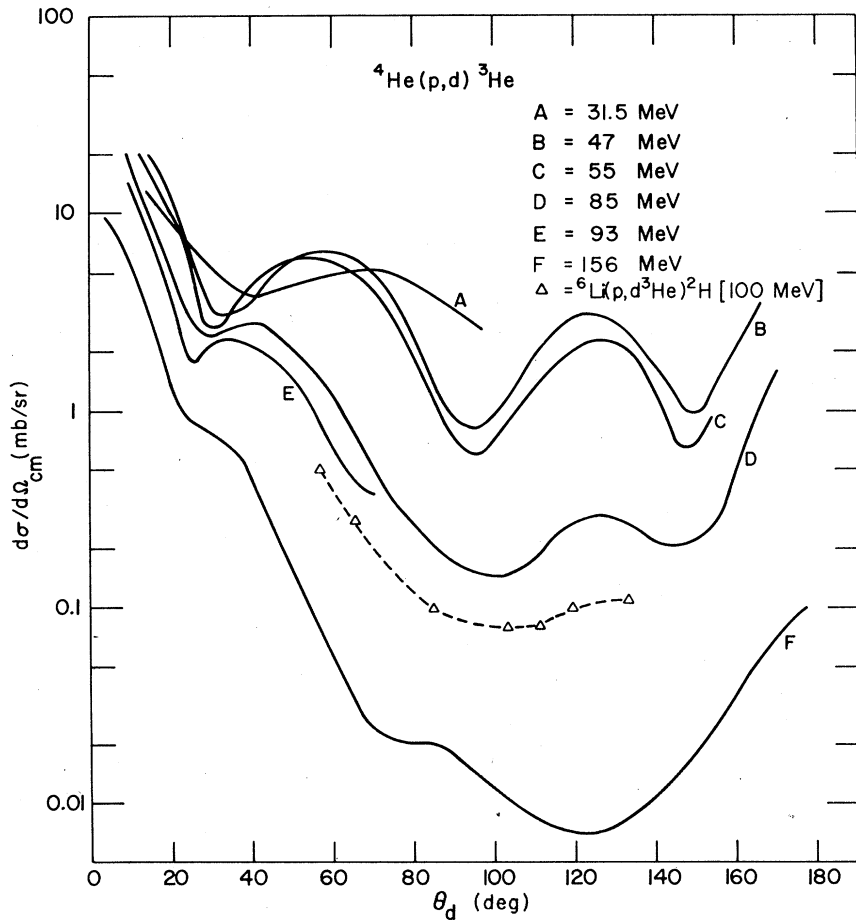


FIG. 9. Quasifree angular distribution for the ${}^6\text{Li}(p, d^3\text{He}){}^2\text{H}$ reaction at 100 MeV. The data points (Δ) represent $(d^3\sigma/d\Omega_d d\Omega_{3\text{He}} dE_d)/K.F.$ at $p_B \approx 0$ MeV/c for various angle pairs plotted versus the two-body center-of-mass scattering angle. The solid curves are smooth curves drawn through the available ${}^4\text{He}(p, d){}^3\text{He}$ data (see Ref. 11). The absolute normalization of the quasifree angular distribution is based on interpolation of the (p, d) data.

A. DWIA parameterization

In the DWIA code the α -particle bound state wave function, which represents a complicated overlap integral between the internal wave functions of the initial and final state nuclei, is approximated by an α particle bound in a Woods-Saxon well with a depth chosen to reproduce the α -particle separation energy. The parameters of this well are taken from the $(p, p\alpha)$ analysis and are listed in Table I. As discussed in Ref. 1 the $1p$ harmonic oscillator shell model suggests the quantum numbers $2S$ for ${}^6\text{Li}$, $2P$ for ${}^7\text{Li}$, and $3S$ for ${}^9\text{Be}$ and ${}^{12}\text{C}$.

For the incident proton we have used the same optical potentials as previously.¹ For the emitted deuteron we have followed the approach of Watanabe,¹¹ who writes the deuteron potential as

$$U_d(r) = \int d\vec{s} [U_p(r_p) + U_n(r_n)] \phi_d^2(s), \quad (5)$$

where only the S -wave part of ϕ_d , the deuteron ground state wave function, is considered. In Eq. (5) for the deuteron potential the position of the center of mass of the deuteron is $\vec{r} = \frac{1}{2}(\vec{r}_n + \vec{r}_p)$, with $\vec{s} = \vec{r}_n - \vec{r}_p$. The optical potentials U_p

and U_n for protons and neutrons are required at approximately half the deuteron energy. For these nucleon potentials we have taken the exit proton optical model potential from our $(p, p\alpha)$ analysis and scaled the well depth using the appropriate energy dependence for this energy region. This approach leads to potentials quite similar to those which actually fit elastic deuteron scattering,¹¹ and it was felt that the use of the nucleon optical potentials from the $(p, p\alpha)$ analysis would provide a more systematic comparison of the two reactions. The deuteron potential calculated by means of this method deviates very slightly from a Woods-Saxon form. For the actual DWIA calculation it was necessary to use an "equivalent" Woods-Saxon deuteron potential which has the same half radius, rms radius, and volume integral as the folded potential. Finally, for the exit ${}^3\text{He}$ particle we have tried two different potentials. Firstly, we have used a potential obtained from analyses¹²⁻¹⁴ of ${}^3\text{He}$ elastic scattering from ${}^6\text{Li}$, ${}^3\text{H}$, and ${}^2\text{H}$. Secondly, we have used the same potential as was used for the α particle in the $(p, p\alpha)$ analysis. We argue that these choices represent the largest reasonable variation possible for the ${}^3\text{He}$ potential. In fact, differ-

TABLE I. Optical potential parameters. The optical potential is defined as follows:

$$V_{\text{opt}} = -Vf(r, r_0, a) - i(W - 4W_p a' \frac{d}{dr'}) f(r, r_0', a') + V_{\text{Coul}},$$

where

$$f(r, r_0, a) = \left[1 + \exp\left(\frac{r - r_0 A^{1/3}}{a}\right) \right]^{-1};$$

A is the target mass, V_{Coul} is the Coulomb potential of a uniform sphere of charge of radius $r_0 A^{1/3}$.

Reaction	System	V	r_0	a	r_c	W	W_d	r_0'	a'	Ref.
${}^6\text{Li}(p, d^3\text{He})^2\text{H}$	$p + {}^6\text{Li}^a$	16.6	1.16	0.75	1.80	0.1	3.9	1.37	0.63	1
	$d + {}^2\text{H}$	6.68	1.66	0.69	1.60	3.2	0	1.66	0.69	
	${}^3\text{He} + {}^2\text{H}$	80.5	1.20	0.70	1.30	0	8.9	1.20	0.65	14
	Bound state	77.0	1.47	0.71	1.47					1
${}^7\text{Li}(p, d^3\text{He})^3\text{H}$	$p + {}^7\text{Li}^a$	17.5	1.33	0.65	1.83	11.6	0	1.46	0.44	1
	$d + {}^3\text{H}$	27.2	1.39	0.52	1.30	0	4.2	1.32	0.62	
	${}^3\text{He} + {}^3\text{H}$	215.0	1.25	0.58	1.40	20.0	0	1.82	0.20	13
	Bound state	91.9	1.43	0.72	1.43					1
${}^9\text{Be}(p, d^3\text{He})^5\text{He}$	$p + {}^9\text{Be}^a$	19.3	1.33	0.65	1.89	10.5	0	1.46	0.44	1
	$d + {}^5\text{He}$	58.4	1.35	0.90	1.30	0	5.8	1.17	0.73	
	${}^3\text{He} + {}^5\text{He}$	82.7	1.20	0.77	1.40	18.4	0	1.67	0.73	12
	Bound state	89.3	1.35	0.73	1.35					1
${}^{12}\text{C}(p, d^3\text{He})^8\text{Be}$	$p + {}^{12}\text{C}^a$	21.2	1.33	0.65	1.33	6.5	0	1.46	0.44	1
	$d + {}^8\text{Be}$	63.2	1.29	0.80	1.30	0	3.8	1.15	1.06	
	${}^3\text{He} + {}^8\text{Be}$	82.7	1.20	0.77	1.40	18.4	0	1.67	0.73	12
	Bound state	89.9	1.23	0.75	1.23					1

^aThese well depths were multiplied by B/A in order to exclude crudely the interaction of the incoming proton with the α cluster.

ences between these two potentials have very little effect on the shape of the cross section and affect the magnitude by less than 15% for all targets. We therefore present only the results for the ^3He potential.

All potential parameters are presented in Table I. For most calculations these parameters were fixed independent of the outgoing energy. Calculations, in which well depths were varied to account for the energy dependence, showed relatively small effects on the shape compared with the experimental errors.

B. Comparison with experimental data

In Fig. 3 we present the DWIA calculations normalized to the experimental data for one pair of angles (for all nuclei except carbon these angles correspond to the double quasifree angle). Agreement between experiment and theory at other angle pairs is of comparable quality. Owing to the lack of experimental $^4\text{He}(p,d)^3\text{He}$ data we have used a constant cross section $d\sigma/d\Omega|_{p=d}$ in Eq. (1). This cross section was obtained by interpolation of the available data presented in Fig. 6 at a two-body angle corresponding to the zero recoil momentum point. Although the free (p,d) data are sparse, the proximity of the present data to the 85 MeV results allows us to interpolate the two-body cross section to an expected accuracy of better than $\pm 25\%$.

Overall, the agreement in shape between experiment and DWIA theory is rather good. However, for ^6Li the theoretical curve is similar to the corresponding $(p,p\alpha)$ predictions whereas one sees in Fig. 5(a) that the $^6\text{Li}(p,p\alpha)$ distribution is narrower than the $(p,d^3\text{He})$ results. Thus for $^6\text{Li}(p,d^3\text{He})$ the theoretical curve is somewhat narrower than experiment unlike the corresponding $(p,p\alpha)$ results. In the case of ^7Li we observe that the almost complete filling in of the expected minimum is not reproduced by the DWIA calculation. This is a somewhat disappointing result, and it seems unlikely that it could be explained as a simple distortion effect. The effects of the finite experimental energy and angular resolution on the theoretical curve were included by means of the code MOMRATH,¹⁵ and are presented as a dashed curve in Fig. 3(b). The majority of the effect arises from the angular resolution, with only an additional few per cent effect from the 1 MeV energy resolution. The inclusion of these finite resolution effects accounts for only about 50% of the observed discrepancy between theory and experiment in the region of the minimum. It is possible that these results indicate the presence of some higher order process not subject to the

same angular momentum transfer requirements.

The $^9\text{Be}(p,d^3\text{He})^5\text{He}$ results presented in Fig. 3(c) are in very good agreement, including a slight improvement when one includes equal amounts of S-state and D-state knockout as predicted by the shell model calculations of Kurath.¹⁶ Finally for $^{12}\text{C}(p,d^3\text{He})^8\text{Be}(0+)$ the agreement between theory and experiment is reasonable when one considers the rather large experimental errors.

In normalizing the DWIA calculation to the experiment we extract the α -particle spectroscopic factor S_α . In common with our earlier analyses of $(p,p\alpha)$ reactions these are absolute spectroscopic factors. In Table II we present the extracted S_α for the angle pairs shown in Fig. 3. In addition we present the extracted S_α for the $(p,p\alpha)$ experiment¹ at these same angle pairs. The errors in S_α represent statistical and relative experimental errors, but do not include any error in the two-body cross sections. Considering the expected uncertainty of approximately $\pm 25\%$ from the interpolation of the two-body cross sections, the agreement between the two experiments is remarkably good.

For completeness we have also presented in Table II theoretical predictions of S_α . The theoretical spectroscopic factors for ^6Li and ^7Li were obtained from cluster model calculations^{17,18} and have large α parentage as expected. As discussed in detail in Ref. 15 the experimental spectroscopic factor for ^6Li is smaller than that predicted by the cluster model suggesting the importance of other configurations. The ^7Li data, however, are in excellent agreement with the cluster model

TABLE II. Absolute spectroscopic factors for double quasifree angle pairs extracted by means of the DWIA analysis. The errors in the spectroscopic factors extracted for the $(p,d^3\text{He})$ reaction only reflect relative errors in the three-body cross sections. An additional estimated uncertainty of $\pm 25\%$ in the $^4\text{He}(p,d^3\text{He})$ cross section should be considered.

Reaction	θ_1/θ_2 (deg)	S_α (expt.)	S_α (theory)
$^6\text{Li}(p,d^3\text{He})^2\text{H}$	81.9/-40.9	0.52 ± 0.03	$1.0 \rightarrow 1.1^b$
$^6\text{Li}(p,p\alpha)^2\text{H}$	81.9/-40.9	0.59 ± 0.04^a	
$^7\text{Li}(p,d^3\text{He})^3\text{H}$	81.3/-41.0	1.09 ± 0.11	
$^7\text{Li}(p,p\alpha)^3\text{H}$	81.3/-41.0	0.94 ± 0.07^a	1.12^c
$^9\text{Be}(p,d^3\text{He})^5\text{He}$	81.2/-41.0	0.47 ± 0.04	
$^9\text{Be}(p,p\alpha)^5\text{He}$	81.2/-41.0	0.43 ± 0.04	0.57^d
$^{12}\text{C}(p,d^3\text{He})^8\text{Be}(0+)$	90/-35.7	0.56 ± 0.12	
$^{12}\text{C}(p,p\alpha)^8\text{Be}(0+)$	90/-35.7	0.59 ± 0.09^a	0.55^d

^a Values from Ref. 1.

^b Reference 17.

^c Reference 18.

^d Reference 16.

prediction.

The spectroscopic factors for ^9Be and ^{12}C were obtained from the shell model calculations of Kurath.¹⁶ They were obtained by projecting out four particles coupled to $S=0$ and $T=0$, having zero oscillator quanta in their relative motion, from $1p$ -shell model wave functions. The agreement between the experimental and theoretical spectroscopic factors is excellent, and shows no evidence of the need for additional clustering beyond that contained in the $1p$ -shell model. These results in terms of the $(p, p\alpha)$ experiment have been discussed in detail in Ref. 1.

VI. CONCLUSIONS

In the present work we have made a detailed study of the $(p, d^3\text{He})$ reaction at 100 MeV. The data generally show the qualitative features expected of a quasifree reaction proceeding via the (p, d) interaction with an α cluster in the target nucleus. Furthermore, comparisons of the experimental data with both $(p, p\alpha)$ experimental data and DWIA calculations show rather good quantitative agreement. In particular within the accuracy of the present work the $(p, d^3\text{He})$ reaction appears to be dominated by the direct quasi-

free reaction. With the possible exception of the filling in of the minimum for ^7Li , no strong evidence (beyond the approximately $\pm 25\%$ uncertainty in the S_α due to the two-body (p, d) data) is seen for other types of processes not contained in the DWIA or for differences in the proton-four-particle cluster interaction between $(p, p\alpha)$ and $(p, d^3\text{He})$. More detailed experimental data will be required if these effects are to be observed. Thus we conclude that the $(p, d^3\text{He})$ reaction on p -shell nuclei is dominated by the quasifree reaction process, and that absolute α -particle spectroscopic factors can be extracted from this reaction via the use of a DWIA analysis.

ACKNOWLEDGMENTS

The authors would like to thank Dr. H. G. Pugh, Dr. R. A. J. Riddle, and Dr. S. M. Smith for useful discussions based on their observations of a quasifree reaction at the Maryland cyclotron prior to this work. We gratefully acknowledge the support of the entire cyclotron staff during these studies. Finally, we are indebted to the University of Maryland Computer Science Center for their generous allocation of computer time for the DWIA calculations.

*Work supported in part by U.S.E.R.D.A.

†On leave of absence from the Council for Scientific and Industrial Research, Pretoria, South Africa.

‡Present address: Athens, Georgia.

¹P. G. Roos *et al.*, Phys. Rev. C **15**, 69 (1977).

²N. S. Chant and P. G. Roos, Phys. Rev. C **15**, 57 (1977).

³M. Furic *et al.*, Phys. Lett. **39B**, 629 (1972).

⁴J. Y. Grossjordan *et al.*, Phys. Rev. Lett. **32**, 173 (1974).

⁵I. Šlaus *et al.*, Phys. Rev. C **8**, 444 (1973); R. G. Allas *et al.*, *ibid.* **9**, 787 (1974).

⁶P. G. Roos and N. S. Chant, in *Proceedings of the Second International Conference on Clustering Phenomena in Nuclei, College Park, Maryland, 1975*, edited by D. A. Goldberg, J. B. Marion, and S. J. Wallace (ERDA Technical Information Center, Oak Ridge, Tennessee), p. 242.

⁷V. V. Balashov, *Proceedings of the Second International Conference on Clustering Phenomena in Nuclei, College Park, Maryland, 1975* (see Ref. 6), p. 281.

⁸N. S. Chant and P. G. Roos, *Proceedings of the Second International Conference on Clustering Phenomena in Nuclei, College Park, Maryland, 1975* (see Ref. 6), p. 265.

⁹P. Frisbee and N. R. Yoder, University of Maryland

Technical Report No. 73-043 (unpublished).

¹⁰The $^4\text{He}(p, d)^3\text{He}$ data at various energies were taken from the following: (31.5 MeV), S. M. Bunch, H. H. Forster, and C. C. Kim, Nucl. Phys. **53**, 241 (1964); (46.8 MeV), J. G. Rogers *et al.*, *ibid.* **A136**, 433 (1969); (55 MeV), S. Hayakawa *et al.*, J. Phys. Soc. Jpn. **19**, 2004 (1964); (85 MeV), L. G. Votta, P. G. Roos, N. S. Chant, and R. Woody, III, Phys. Rev. C **10**, 520 (1974); (93 MeV), W. Selove and J. M. Teem, Phys. Rev. **112**, 1658 (1958); (156 MeV), M. Bernas *et al.*, Phys. Lett. **25B**, 260 (1967).

¹¹Shiguo Watanabe, Nucl. Phys. **8**, 484 (1958); F. G. Perey and G. R. Satchler, *ibid.* **A97**, 515 (1967).

¹²C. C. Chang (private communication).

¹³P. G. Roos *et al.*, Nucl. Phys. **A257**, 317 (1976); E. E. Gross *et al.*, Phys. Rev. C **5**, 602 (1972).

¹⁴F. Hinterberger *et al.*, Nucl. Phys. **A111**, 265 (1968).

¹⁵Finite resolution effects were calculated with the code MOMRATH, J. W. Watson (private communication).

¹⁶D. Kurath, Phys. Rev. C **7**, 139 (1973).

¹⁷I. V. Kurdyumov, V. G. Neudatchin, and Yu. F. Smirnov, Phys. Lett. **31B**, 426 (1970).

¹⁸Yu. F. Smirnov and D. Chlebowska, Nucl. Phys. **26**, 306 (1961).